Radiative Corrections to SIDIS: Current Status and Perspectives

Igor Akushevich
Duke University, Durham, NC USA



in collaboration with
Haiyan Gao, Sasha Ilyichev,
Vlad Khachatryan, Youjie Lin, Tianbo Liu,
and W. Melnitchouk

e-mail: igor.akushevich@duke.edu

Introduction and Outline

- SIDIS is a primary tool for extracting multidimensional nucleon structure, including TMDs and fragmentation functions.
- The precision achieved at JLab and expected at the EIC requires radiative-correction calculations beyond the traditional level of accuracy.
- This motivates a reexamination of SIDIS radiative corrections, their theoretical foundations, higher-order contributions, and associated systematic uncertainties.

Outline

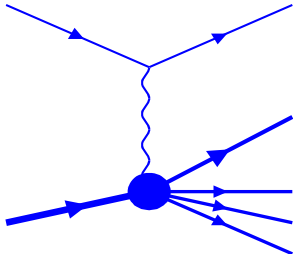
- Traditional approaches to SIDIS radiative corrections
- A hybrid framework: combining the strengths of traditional and factorized approaches
- A factorization framework based on Exact Physical Matching (EPM)
- Radiative azimuthal mixing and its phenomenological implications
- Open theoretical questions and future directions

Part II:

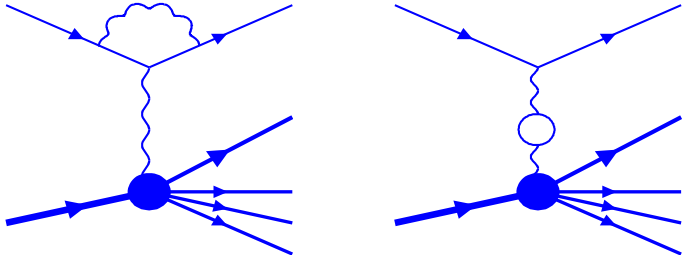
Traditional Approaches to SIDIS Radiative Corrections

Contribution to RC in SIDIS

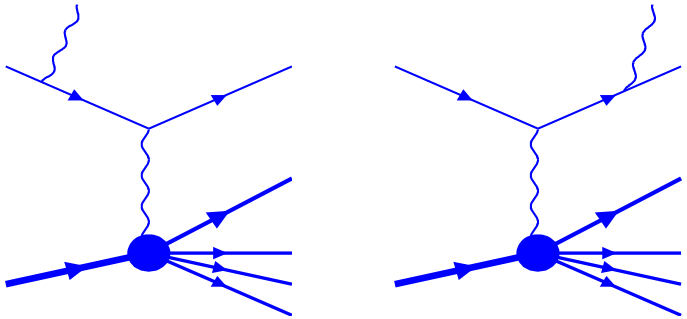
The Born cross section



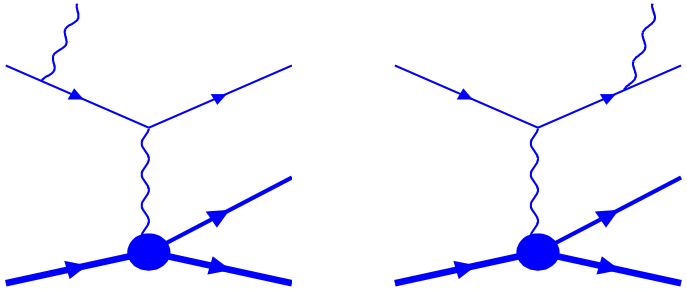
Loop diagrams



Emission of a radiated photon (semi-inclusive processes)



Emission of a radiated photon (exclusive processes)



Current Status of Our Calculations

- RC to unpolarized SIDIS cross section, angular structure
  - Akushevich I, Shumeiko N, and Soroko A (1999) Radiative effects in the processes of hadron electroproduction. *European Physical Journal*, C10(4), pp.681-687.
- Radiative tail from exclusive peak
  - Akushevich I, Ilyichev A, and Osipenko M (2009) Lowest order QED radiative corrections to five-fold differential cross section of hadron leptoproduction. *Physics Letters* B672(1), pp.35-44.
- General calculation of RC for polarized particles
  - Akushevich I and Ilyichev A (2019) Lowest order QED radiative effects in polarized SIDIS. *Physical Review* D100(3), p.033005.
- Leading Log and the best approximation
  - Akushevich I, Srednyak S, and Ilyichev A (2024) Exact and leading order radiative effects in semi-inclusive deep inelastic scattering. *Physical Review* D109(7), p.076028.
- Radiative tail from exclusive peak
  - Akushevich I, Avakian H, Ilyichev A, Srednyak S (2023) Complete lowest order radiative corrections in semi-inclusive scattering of polarized particles. *The European Physical Journal* A59(10), 246.

Exact Formulae for RC in SIDIS

The total RC is calculated exactly in our paper (PR D100 (2019) 033005):

$$\sigma_{RC} = \frac{\alpha}{\pi}\exp(\delta_{inf})\left(\delta_{VR} + \delta^{l}_{vac} + \delta^{h}_{vac}\right)\sigma_B + \sigma^{F}_{R} + \sigma_{AMM} + \sigma^{ex}_{R}$$

Here δ_{VR} and $\delta^{l,h}_{vac}$ come from the radiation of soft photons and the effects of vacuum polarization, the correction δ_{VR} is infrared-free sum of factorized parts of real and virtual photon radiation, and σ^{F}_{R} and σ^{ex}_{R} are contributions from the process of emission of an additional real photon:

$$\begin{aligned}
\sigma_B &= \frac{\alpha^2 S_x^2}{4Q^4\sqrt{\lambda_Y}S}\sum_{i=1}^{9}\theta_i^B\mathcal{H}_i \\
\sigma^{F}_{R} &= -\frac{\alpha^3 S S_x^2}{32\pi^2\lambda_S\lambda_Y}\int\limits_{\tau_{\min}}^{\tau_{\max}}d\tau\int\limits_{0}^{2\pi}d\phi_k\int\limits_{0}^{R_{\max}}dR\sum_{i=1}^{9}\left[\sum_{j=1}^{k_i}\tilde{\mathcal{H}}_i\theta_{ij}\frac{R^{j-2}}{\tilde{Q}^4} - \frac{\theta_{i1}\mathcal{H}_i}{RQ^4}\right], \\
\sigma^{ex}_{R} &= -\frac{\alpha^3 S S_x^2}{2^8\pi^5\lambda_S\lambda_Y}\int\limits_{\tau_{\min}}^{\tau_{\max}}d\tau\int\limits_{0}^{2\pi}d\phi_k\sum_{i=1}^{9}\sum_{j=1}^{k_i}\frac{\tilde{\mathcal{H}}^{ex}_i\theta_{ij}R_{ex}^{j-2}}{(1+\tau-\mu)\tilde{Q}^4}.
\end{aligned}$$

Explicit expressions for the functions θ_{ij} are given in Appendix B of our paper.

Leading, Next-to-Leading, and Exact Contributions to RC

By “exactly” calculated RC we understand the estimation of the lowest order RC contribution with any predetermined accuracy. The structure of the dependence on the electron mass in RC cross section:

$$\sigma_{RC} = A \log \frac{Q^2}{m^2} + B + O(m^2/Q^2)$$

where A and B do not depend on the electron mass m.

- If only A is kept, this is the leading log approximation.
- If both contributions are kept (i.e., contained A and B), this is the calculation with the next-to-leading accuracy, practically equivalent to exact calculation.

Three approaches to extract the leading Log contribution for the SIDIS cross section (i.e., to calculate A)

- use our exact formulae, collect all terms that result in leading log after integration over photon angles, combine them into the final expression
- extract the poles that correspond to radiation collinear to initial and final electron, integrate over angles, and find the factorizing form traditional for leading log calculations.
- use the method of the electron structure functions.

Leading Log: Extraction from Exact Formulae

The exact expression for σ_R^F is:

$$\sigma_R^F = -\frac{\alpha^3 S S_x^2}{32\pi^2 \lambda_S \lambda_Y} \int_{\tau_{\min}}^{\tau_{\max}} d\tau \int_0^{2\pi} d\phi_k \int_0^{R_{\max}} dR \sum_{i=1}^{9} \left[\sum_{j=1}^{k_i} \tilde{\mathcal{H}}_i \theta_{ij} \frac{R^{j-2}}{\tilde{Q}^4} - \frac{\theta_{i1} \mathcal{H}_i}{R Q^4} \right],$$

Analysis of the integrand and tracing the origin of the leading log allows us to extract the leading log terms from the exact formulae:

$$\int_{\tau_{\min}}^{\tau_{\max}} d\tau \int_0^{2\pi} d\phi_k \sum_{j=1}^{k_i} \theta_{ij}^s R^{j-2} = -4\pi l_m \frac{\sqrt{\lambda_Y}}{S} \frac{1+z_1^2}{z_1(1-z_1)} \theta_i^{Bs}$$

$$\int_{\tau_{\min}}^{\tau_{\max}} d\tau \int_0^{2\pi} d\phi_k \sum_{j=1}^{k_i} \theta_{ij}^p R^{j-2} = -4\pi l_m \frac{\sqrt{\lambda_Y}}{X} \frac{1+z_2^2}{1-z_2} \theta_i^{Bp}$$

Leading Log: Exclusive Radiative Tail

Exact contribution calculated inour 2019 paper is:

$$\sigma_R^{ex} = -\frac{\alpha^3 S S_x^2}{2^8\pi^5\lambda_S\lambda_Y}\int_{\tau_{\min}}^{\tau_{\max}} d\tau \int_0^{2\pi} d\phi_k \sum_{i=1}^{9}\sum_{j=1}^{k_i} \frac{\tilde{\mathcal{H}}_i^{ex}\theta_{ij}R_{ex}^{j-2}}{(1+\tau-\mu)\tilde{Q}^4}.$$

where $R_{ex} = \frac{p_x^2 - m_u^2}{1+\tau-\mu}$. The Born cross section of exclusive process is:

$$\sigma_{ex}^B = \frac{\alpha^2 S_x}{32\pi^3 Q^4 S\sqrt{\lambda_Y}}\sum_{i=1}^{9}\mathcal{H}_i^{ex}\theta_i^B$$

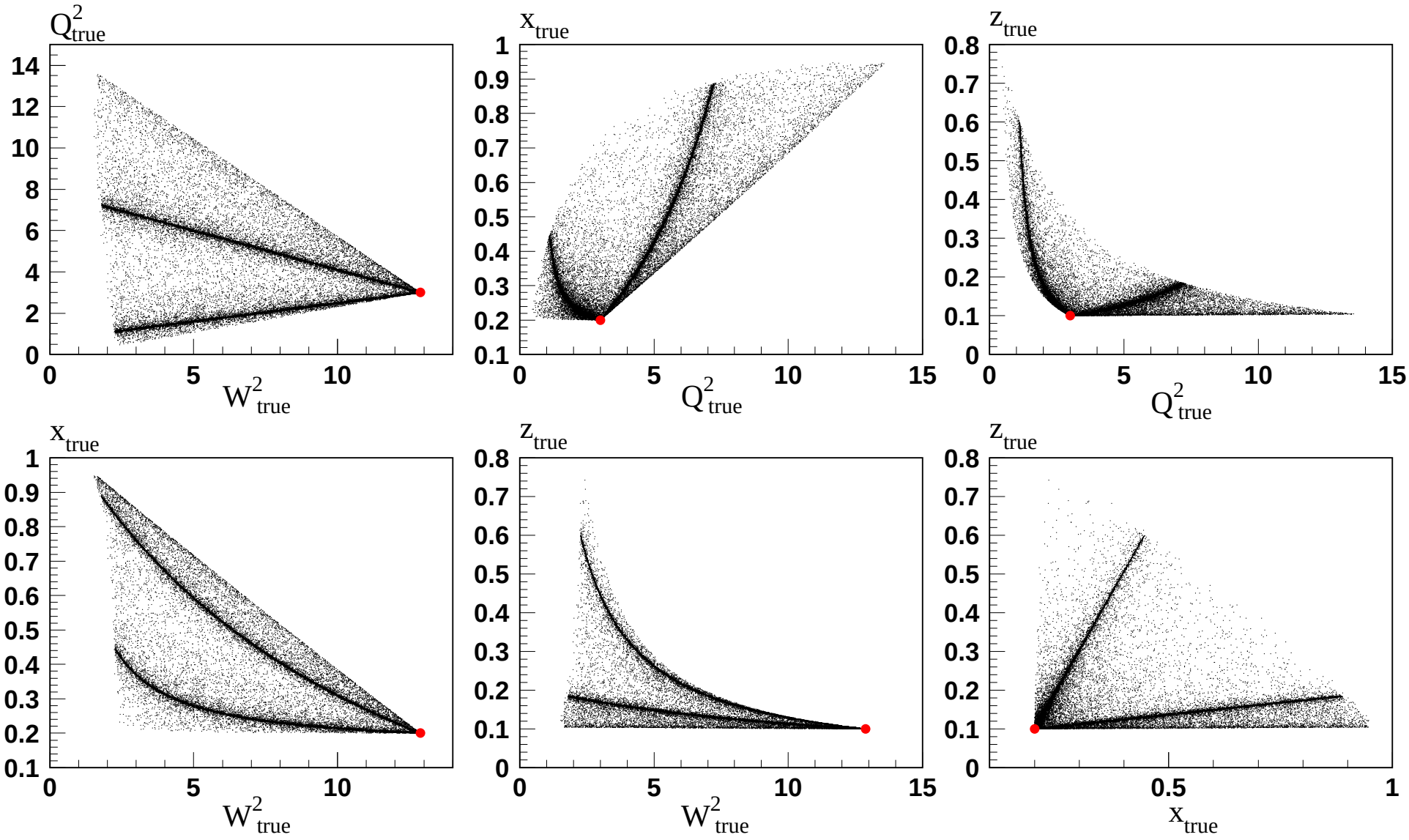
Therefore we have

$$\sigma_{sex}^1 = \frac{\alpha}{2\pi} l_m \sqrt{\frac{\lambda_Y^{se}}{\lambda_Y}}\frac{S_x^2}{S' S_x^{se}}\frac{1+z_{1ex}^2}{1-z_{1ex}}\sigma_{sex}^B,$$

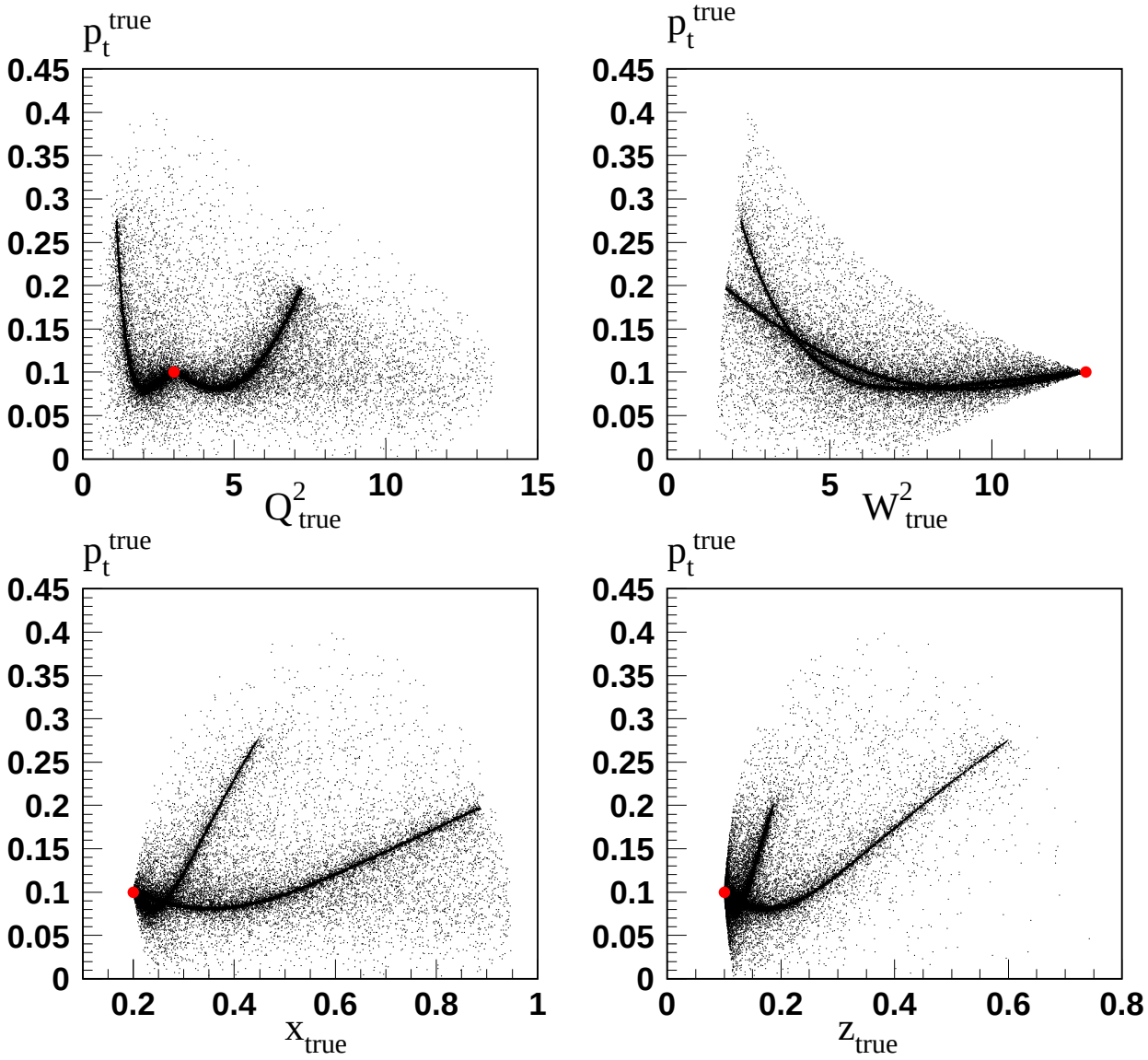
$$\sigma_{pex}^1 = \frac{\alpha}{2\pi} l_m \sqrt{\frac{\lambda_Y^{pe}}{\lambda_Y}}\frac{S_x^2}{X' S_x^{pe}}\frac{1+z_{2ex}^2}{1-z_{2ex}}\sigma_{pex}^B,$$

where $z_{1ex} = 1-(p_x^2-m_u^2)/S'$ and $z_{2ex} = (1+(p_x^2-m_u^2)/X')^{-1}$.

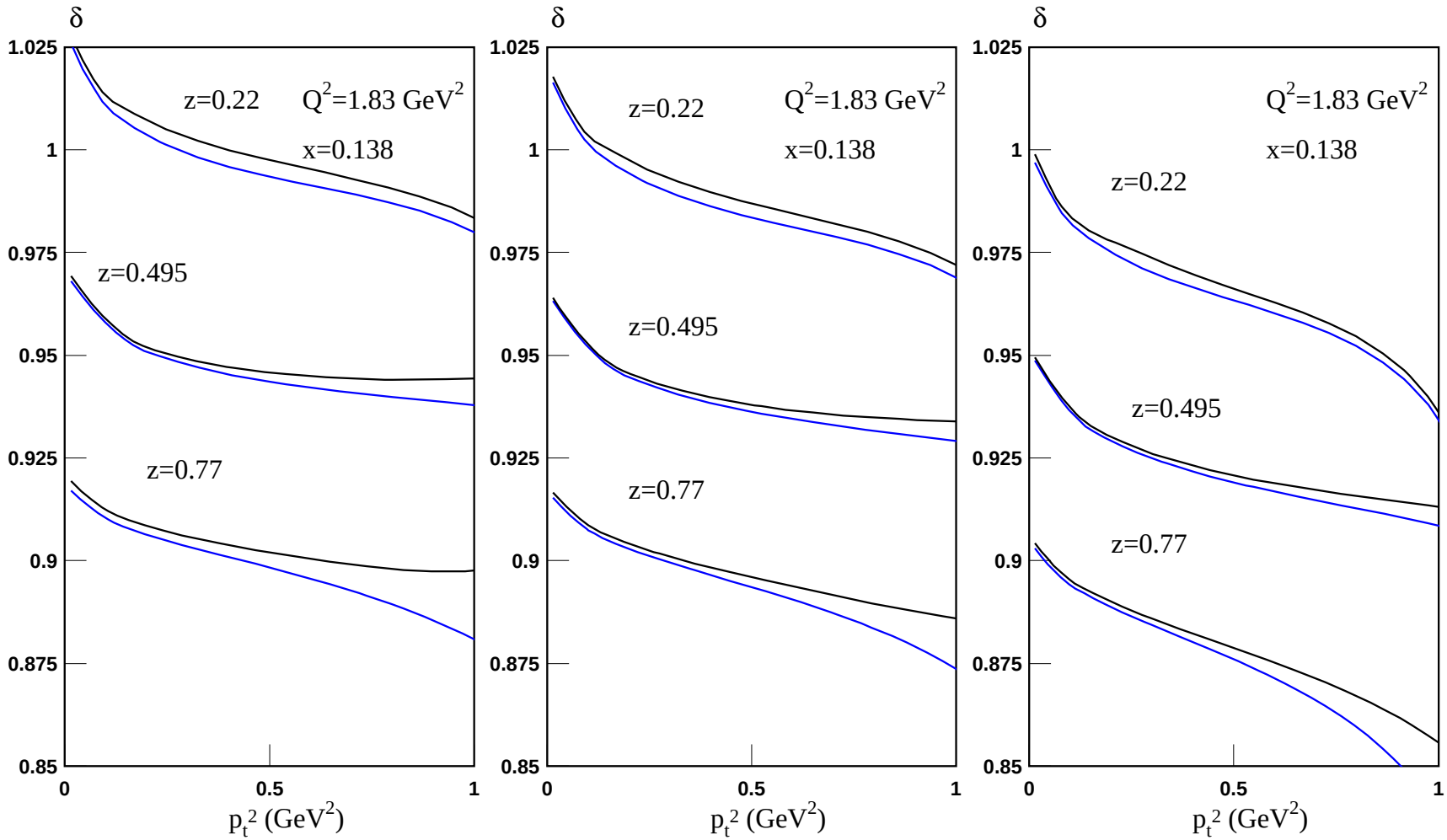
Kinematic Regions for SIDIS SFs (x,Q2,W2,z)



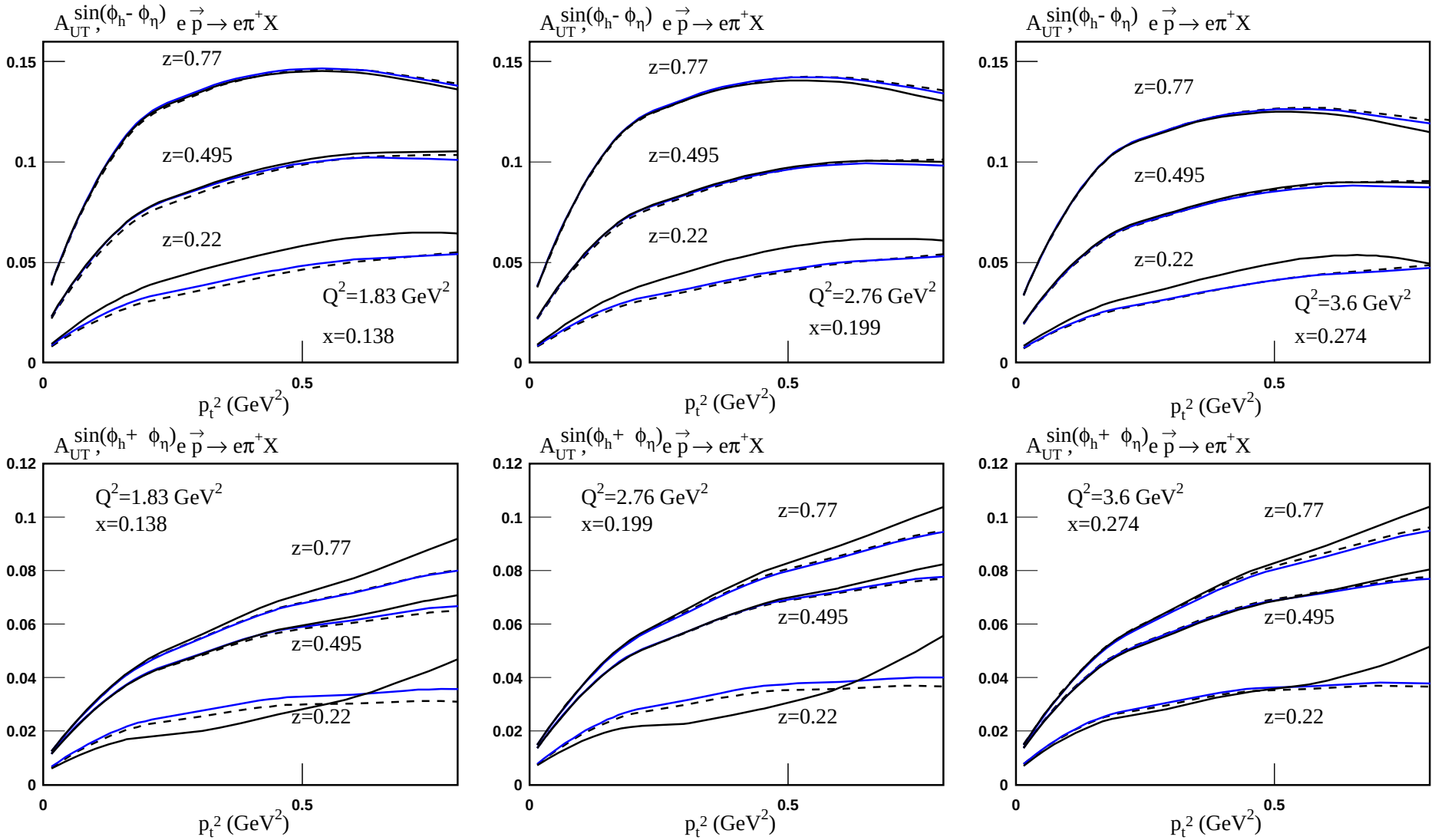
Kinematic Region for SIDIS SFs (pt)



RC to Unpolarized Cross Section



RC to Collins and Sivers Asymmetries



Part III:

A Hybrid Framework: Combining the Strengths of Traditional and Factorized Approaches

Hybrid Approach: Motivation and Goal

- Precision SIDIS measurements require accurate treatment of QED radiative effects.
- Two conceptually different frameworks are currently available:
  - Traditional approach: exact $\mathcal{O}(\alpha)$ radiative corrections + ESF resummation.
  - Factorized approach: LDF/LFF factorization with perturbative evolution.
- Both frameworks aim to describe the same physical cross section.
- The relation between their predictions is not completely understood.
- Goal: understand similarities, differences, and domains of applicability.

Main questions:

- Formulate the traditional and factorized computational schemes.
- Identify the universal LL contributions in both approaches.
- Compare the resulting LL approximations analytically.
- Compare LL+NL contributions at lowest and higher orders numerically.
- Determine the theoretical origin of the observed discrepancies.

I. Akushevich, H. Gao, A. Ilyichev, S. Jia, V. Khachatryan, Y. Lin, T. Liu, and W. Melnitchouk, "QED radiative effects in semi-inclusive deep-inelastic scattering: traditional and factorized approaches," arXiv:2608.20294 [hep-ph] (2026).

Traditional and Factorized Approaches

Traditional approach $\sigma_{\rm RC} = \sigma_B + \sigma_V + \sigma_R + \sigma_{\rm ERT}$

- Exact treatment of real and virtual corrections.
- Explicit phase-space integration.
- Infrared cancellation performed before final integration.
- Electron structure functions for higher-order RC in LL.
- Exclusive radiative tail treated separately.

Factorized approach $\sigma = D_i \otimes H \otimes D_f$

- Universal lepton distribution and fragmentation functions.
- Convolution of LDFs/LFFs with the hard scattering cross section.
- QED and QCD radiation treated within the same framework.
- Mellin-space evolution and all-order resummation of collinear logarithms.
- Natural implementation of higher-order corrections.

The two approaches are based on different factorization and resummation strategies. Their relation at leading and nonleading orders is the subject of the present comparison.

Factorized Approach

$$\frac{\mathrm{d}^6\sigma^{\mathrm{obs}}}{\mathrm{d}x\,\mathrm{d}y\,\mathrm{d}\phi\,\mathrm{d}z\,\mathrm{d}\phi_h\,\mathrm{d}p_t^2} = \int_{\xi_{\mathsf{min}}}^1 \mathrm{d}\xi\, f_{e/e}(\xi,Q^2) \int_{\zeta_{\mathsf{min}}(\xi)}^1 \mathrm{d}\zeta\, D_{e/e}(\zeta,Q^2)\, \widehat{J}\, \frac{\mathrm{d}^6\hat{\sigma}\left(\alpha(Q^2)\right)}{\mathrm{d}\hat{x}\,\mathrm{d}\hat{y}\,\mathrm{d}\hat{\phi}\,\mathrm{d}\hat{z}\,\mathrm{d}\hat{\phi}_h\,\mathrm{d}\hat{p}_t^2}\,,$$

In factorized framework, collinear QED radiation produces large logarithms order by order in perturbation theory. Their resummation is achieved through ESF obeying QED DGLAP evolution equations.

$$\frac{\mathrm{d}f_{i/e}(\xi,Q^2)}{\mathrm{d}\log Q^2} = \frac{\alpha(Q^2)}{2\pi}\sum_j P_{ij}(\xi)\otimes_\xi f_{j/e}(\xi,Q^2),$$

$$\frac{\mathrm{d}D_{e/i}(\zeta,Q^2)}{\mathrm{d}\log Q^2} = \frac{\alpha(Q^2)}{2\pi}\sum_j D_{e/j}(\zeta,Q^2)\otimes_\zeta P_{ji}(\zeta),$$

where $i,j = e,\bar{e},\gamma$, and the symbol $\otimes_x$ denotes the Mellin convolution,

$$\frac{\mathrm{d}^6\sigma^{\mathrm{obs}}_{\mathcal{O}(\alpha),\mathrm{LL+NL}}}{\mathrm{d}x\,\mathrm{d}y\,\mathrm{d}\phi\,\mathrm{d}z\,\mathrm{d}\phi_h\,\mathrm{d}p_t^2} = \frac{\alpha(m^2)}{2\pi}\left[\frac{4}{3}\log\frac{Q^2}{m^2}\,\sigma_B + \int_{\xi_{\mathsf{min}}}^1 \mathrm{d}\xi\left[\frac{1+\xi^2}{1-\xi}\left(\log\frac{Q^2}{(1-\xi)^2m^2}-1\right)\right]_+ \widehat{J}\,\hat{\sigma}_B\Big|_{\zeta=1}\right.$$
$$\left. + \int_{\zeta_{\mathsf{min}}(1)}^1 \mathrm{d}\zeta\left[\frac{1+\zeta^2}{1-\zeta}\left(\log\frac{Q^2}{(1-\zeta)^2m^2}-1\right)\right]_+ \widehat{J}\,\hat{\sigma}_B\Big|_{\xi=1}\right].$$

Analytical and Numerical Comparison

- Analytical comparison showed coincidence of the Born cross section and the lowest order RC. Specifically, the exact coincidence was found for:
  - the structure of the cross sections and vacuum polarization corrections,
  - expressions for shifted variables that are argument of the Born cross section in the integrands,
  - expressions for Jacobian transformation, lower integration limits, and splitting functions.
- Numeric comparison was performed for kinematical conditions of JLab, HERMES, and EIC
  - Excellent agreement at Born and LL level was found for both unpolarized cross section and spin asymmetries.
  - Differences become visible when finite nonleading contributions are included.
  - For unpolarized π^+ electroproduction cross sections, the discrepancies reach approximately

$$2\% \quad (\mathrm{JLab}), \qquad 7\% \quad (\mathrm{HERMES}), \qquad 5\% \quad (\mathrm{EIC}).$$

  - Similar effects are observed for Collins and Sivers asymmetries.

The next question is:

What is the origin of these differences?

Origin of the Difference

Observations:

- The discrepancy originates entirely from finite nonleading contributions.
- In the factorized approach these contributions enter through the perturbative initial conditions of the LDFs and LFFs.
- The dominant effect is associated with terms proportional to $P(z)\ln(1-z)$.
- Numerically, the $P(z)\log(1-z)$ contribution accounts for most of the observed differences between the approaches.

For example, the perturbative initial condition of the LDF is

$$f_{0,e/e}(z) = \delta(1-z) + \frac{\alpha}{2\pi}\left[\frac{1+z^2}{1-z}\left(\frac{1}{\epsilon} + \ln\frac{\mu_R^2}{(1-z)^2 m^2} - 1\right)\right]_+ .$$

The factor $(1-z)^2 m^2$ in the logarithm generates finite contributions proportional to

$$P(z)\ln(1-z).$$

Although formally nonleading, this term provides the dominant source of the analytical and numerical differences observed in the comparison.

Physical Interpretation

In the factorized approach, the transverse-momentum integration is performed independently of the kinematic constraints of a particular process (i.e., from 0 to ∞) and generates $\log(1-z)$

$$\int_0^\infty \frac{dk_T^2}{k_T^2+(1-z)^2m^2} \;\to\; \ln\frac{\mu_R^2}{(1-z)^2m^2} = \ln\frac{\mu_R^2}{m^2} - 2\ln(1-z).$$

In an explicit radiative-correction calculation, the integration is performed with physical phase-space boundaries, $k_{T,\max}^2(z) = Q^2(1-z)^2/4z$,

$$\int_0^{k_{T,\max}^2(z)} \frac{dk_T^2}{k_T^2+(1-z)^2m^2} = \ln\left(1+\frac{Q^2}{4zm^2}\right),$$

- Universal factorization requires transverse-momentum integrations to be defined independently of process-specific kinematic boundaries, implying an extension of the upper integration limit to $k_T^2 = \infty$.
- The resulting discrepancy reflects the incompatibility between exact kinematics and the universality principle of operator-based factorization.

Hybrid Approach: Conclusions

- Traditional and factorized approaches provide a consistent description of SIDIS radiative effects at the leading-logarithmic level.
- Numerical differences originate from finite subleading contributions.
- The largest effect is associated with $\log(1-z)$ terms appearing in perturbative LDF/LFF initial conditions.
- These terms are factorization-scheme dependent and should be interpreted within a complete factorized calculation.
- A combined or hybrid framework may exploit the strengths of both approaches.

Key message:
The comparison clarifies both the common physical foundation of the two approaches and the origin of their observed differences.

Moreover, these results motivate a closer examination of factorization-scheme freedom and provide the motivation for the Exact Physical Matching (EPM) approach.

Part IV:

A Factorization Framework Based on Exact Physical Matching (EPM)

Freedom in Organizing Radiative Corrections

The factorized approach is based on the decomposition

$$\sigma = D_i \otimes H \otimes D_f,$$

where D_i and D_f describe initial- and final-state radiation, while H denotes the hard scattering contribution. Expanding to first order in α,

$$\sigma = \sigma_B + \frac{\alpha}{2\pi}\left[D_i^{(1)} \otimes \sigma_B + \sigma_B \otimes D_f^{(1)} + K\right] + \mathcal{O}(\alpha^2).$$

The physical cross section σ is observable, whereas the separate quantities D_i, D_f, and H are auxiliary theoretical objects. Consequently, the decomposition is not unique. The transformations

$$D_i^{(1)} \to D_i^{(1)} + \Delta_i, \qquad D_f^{(1)} \to D_f^{(1)} + \Delta_f,$$

can be compensated by a redefinition of the hard coefficient,

$$K' = K - \Delta_i \otimes \sigma_B - \sigma_B \otimes \Delta_f,$$

such that $\sigma' = \sigma$.

- Therefore finite contributions may be shifted between ISR, FSR and the hard scattering coefficient without changing the physical cross section.
- Different choices correspond to different factorization schemes.

Examples of Factorization Schemes

The first-order distribution function can be written as

$$D^{(1)}(z, L) = L\,P(z) + R(z), \quad \text{with} \quad L = \ln \frac{Q^2}{m_e^2}, \quad \text{and} \quad P(z) = \left(\frac{1+z^2}{1-z}\right)_+ .$$

The logarithmic contribution $LP(z)$ is universal and controls the leading collinear behavior. The finite term $R(z)$ is not uniquely defined and depends on the chosen factorization prescription.

Examples:

- **LL scheme**: $R(z) = 0$, all finite contributions are absorbed into the hard coefficient.
- Δ **scheme** finite terms are incorporated into the distribution functions through a specific subtraction prescription.
- $\overline{\rm MS}$ **scheme** finite terms are fixed by dimensional regularization and $\overline{\rm MS}$ subtraction.
- **EPM scheme** the hard coefficient is defined by the matching condition

$$\sigma^{\rm fact} = \sigma^{\rm exact} + \mathcal{O}(\alpha^2).$$

Thus EPM should be viewed not as a different factorization framework but as a particular factorization scheme based on exact first-order physical matching.

Exact Physical Matching (EPM) Scheme

The exact first-order radiative correction is written as

$$\sigma^{\rm exact} = \sigma_B + \frac{\alpha}{2\pi}\sigma_1^{\rm exact}.$$

The defining principle of EPM is

$$\sigma^{\rm fact} = \sigma^{\rm exact} + \mathcal{O}(\alpha^2).$$

Using the first-order factorized representation,

$$\sigma_1^{\rm exact} = D_i^{(1)} \otimes \sigma_B + \sigma_B \otimes D_f^{(1)} + K_{\rm EPM},$$

which gives

$$K_{\rm EPM} = \sigma_1^{\rm exact} - D_i^{(1)} \otimes \sigma_B - \sigma_B \otimes D_f^{(1)}.$$

Thus the hard coefficient is determined directly from the exact physical first-order correction.

Key ideas:

- Preserve the exact known $\mathcal{O}(\alpha)$ correction.
- Retain the factorized structure.
- Use the exact RC as the starting point for higher orders.
- Reduce scheme arbitrariness.

EPM Factorization Formula and Higher Orders

The EPM factorized cross section is

$$\sigma = D_i \otimes \left(\sigma_B + \frac{\alpha}{2\pi} K_{\rm EPM}\right) \otimes D_f \,.$$

By construction

$$\sigma = \sigma^{\rm exact} + \mathcal{O}(\alpha^2).$$

Properties:

- Exact reproduction of the known $\mathcal{O}(\alpha)$ result.
- Hard coefficient determined by physical matching.
- Preserves the standard ESF framework and LL resummation.
- Reduces arbitrariness in the treatment of finite first-order contributions.
- Provides a physically motivated starting point for higher-order approximations.

Higher-order radiative effects are generated through the electron distribution functions.
Two complementary strategies are:

- Perturbative construction of higher-order corrections
- Mellin-space representation for all-order resummation

Perturbative Construction of Higher-Order Corrections

The factorized cross section is:

$$\sigma_{\rm EPM} = D_i \otimes H_{\rm EPM} \otimes D_f .$$

The electron distribution functions and EPM hard coefficient admit a perturbative expansion

$$D(z,L) = \delta(1-z) + \frac{\alpha}{2\pi} D^{(1)}(z,L) + \left(\frac{\alpha}{2\pi}\right)^2 D^{(2)}(z,L) + \mathcal{O}(\alpha^3),$$

$$H_{\rm EPM} = \sigma_B + \frac{\alpha}{2\pi} K_{\rm EPM}.$$

Proceeding to second order,

$$\sigma_{\rm EPM} = \sigma_B + \frac{\alpha}{2\pi}\sigma_1^{\rm exact} + \left(\frac{\alpha}{2\pi}\right)^2 \sigma_2^{\rm EPM} + \mathcal{O}(\alpha^3),$$

where

$$\sigma_2^{\rm EPM} = D_i^{(2)} \otimes \sigma_B + \sigma_B \otimes D_f^{(2)} + D_i^{(1)} \otimes \sigma_B \otimes D_f^{(1)} + D_i^{(1)} \otimes K_{\rm EPM} + K_{\rm EPM} \otimes D_f^{(1)}.$$

Key observation is that the exact first-order information contained in $K_{\rm EPM}$ contributes not only at $\mathcal{O}(\alpha)$, but propagates into all higher perturbative orders. Thus higher-order corrections inherit the exact physical information used in the matching procedure.

Key message: $\quad$ Exact first order $\quad\Longrightarrow\quad$ Improved higher orders.

Mellin-Space Representation and All-Order Resummation

The perturbative construction has an equivalent Mellin-space representation.

Define Mellin moments by

$$F(N) = \int_0^1 dz\, z^{N-1} F(z).$$

Then convolutions become ordinary products,

$$\sigma_{\rm EPM}(N) = D_i(N)\, H_{\rm EPM}(N)\, D_f(N).$$

The electron distribution functions may be written in exponentiated form,

$$D(N, L) = \exp[\Gamma(N, L)]\,,$$

so that

$$\sigma_{\rm EPM}(N) = e^{\Gamma_i(N,L)}\, H_{\rm EPM}(N)\, e^{\Gamma_f(N,L)}.$$

Properties:

- Mellin-space treatment is identical to the standard factorized approach.
- EPM does not modify the evolution equations or resummation machinery.
- The only modification is the matching condition used to determine the hard coefficient $H_{\rm EPM}$.

EPM Approach: Summary

Main properties of EPM:

- Exact first-order radiative corrections are preserved by construction.
- Finite terms are fixed through physical matching rather than a subtraction prescription.
- Higher-order corrections inherit the exact first-order physical information.
- Standard factorized evolution and resummation machinery remain unchanged.

Therefore

$$\boxed{\text{EPM} = \text{Physical matching} + \text{standard factorized resummation}}$$

rather than a new resummation formalism.

Consequence:

The ambiguity associated with finite scheme-dependent terms, including contributions proportional to $P(z)\ln(1-z)$, is eliminated at $\mathcal{O}(\alpha)$ through exact physical matching.

Part V:

Radiative Azimuthal Mixing

and

its Phenomenological Implications

Radiative Azimuthal Mixing

- At Born level, azimuthal weights project out individual structure functions.
- Example:

$$\langle \sin(\phi_h - \phi_S) \rangle = \int d\phi_h \, d\phi_S \, \sin(\phi_h - \phi_S) \, d\sigma_B \propto F_{UT}^{\sin(\phi_h - \phi_S)}$$

- Photon emission changes the azimuthal structure of the cross section.
- Orthogonality of the Born harmonics is lost.
- The weighted radiative cross section receives contributions from all 18 SIDIS structure functions.

$$\langle \sin(\phi_h - \phi_S) \rangle_R = \int d\phi_h \, d\phi_S \, \sin(\phi_h - \phi_S) \, d\sigma_R = \sum_{i=1}^{18} M_i \, F_i$$

- This phenomenon is called **radiative azimuthal mixing**.

Radiative azimuthal mixing is the loss of the one-to-one correspondence between SIDIS asymmetries and structure functions due to QED radiation.

Sivers and Collins asymmetries

The general definitions and the expressions at the Born level are:

- Sivers asymmetry

$$A_{UT}^{\sin(\phi_h-\phi_\eta)} = \frac{2\int_0^{2\pi} d\phi_\eta \int_0^{2\pi} d\phi_h \sin(\phi_h-\phi_\eta)\sigma^{UT}}{\int_0^{2\pi} d\phi_\eta \int_0^{2\pi} d\phi_h \sigma^{UT}}, \qquad A_{UT}^{\sin(\phi_h-\phi_\eta)} = \frac{F_{UT,T}^{\sin(\phi_h-\phi_\eta)}}{F_{UU,T}}$$

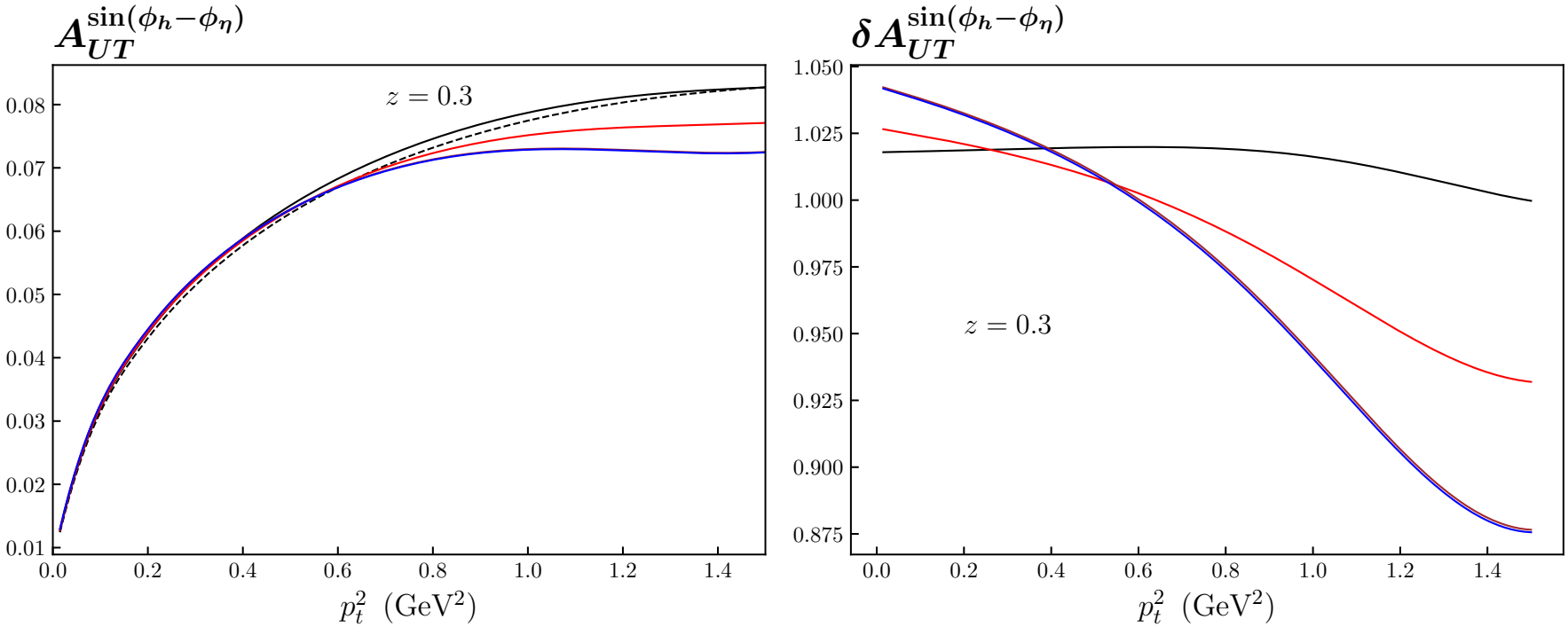
- Collins asymmetry

$$A_{UT}^{\sin(\phi_h+\phi_\eta)} = \frac{2\int_0^{2\pi} d\phi_\eta \int_0^{2\pi} d\phi_h \sin(\phi_h+\phi_\eta)\sigma^{UT}}{\varepsilon\int_0^{2\pi} d\phi_\eta \int_0^{2\pi} d\phi_h \sigma^{UT}}, \qquad A_{UT}^{\sin(\phi_h+\phi_\eta)} = \frac{F_{UT,T}^{\sin(\phi_h+\phi_\eta)}}{F_{UU,T}}$$

Sivers and Collins asymmetries

We added step by step the different contributions in order to see the quantities of the effect

- Basic contributions $F_{UU,T}$ and $F_{UT,T}^{\sin(\phi_h-\phi_\eta)}$ ($F_{UT}^{\sin(\phi_h+\phi_\eta)}$)
- Unpolarized contributions $F_{UU}^{\cos\phi_h}$ and $F_{UU}^{\cos 2\phi_h}$
- Transverse contributions $F_{UT}^{\sin(\phi_\eta)}$, $F_{UT}^{\sin(3\phi_h-\phi_\eta)}$, $F_{UT}^{\sin(2\phi_h-\phi_\eta)}$
- Longitudinal contributions $F_{UL}^{\sin(\phi_h)}$ $F_{UL}^{\sin(2\phi_h)}$.



Born cross section

$$
\begin{aligned}
\frac{d^6\sigma_B}{dx\,dy\,d\phi\,dz\,d\phi_h\,dp_t^2} &= \frac{\alpha^2}{xy\,Q^2}\,\frac{y^2}{2\,(1-\varepsilon)}\left(1+\frac{\gamma^2}{2x}\right)\Bigg\{F_{UU,T}+\varepsilon F_{UU,L} \\
&\quad +\sqrt{2\,\varepsilon(1+\varepsilon)}\,\cos\phi_h\,F_{UU}^{\cos\phi_h}+\varepsilon\cos(2\phi_h)\,F_{UU}^{\cos 2\phi_h} \\
&\quad +\lambda_e\,\sqrt{2\,\varepsilon(1-\varepsilon)}\,\sin\phi_h\,F_{LU}^{\sin\phi_h}+\eta_L\left[\sqrt{2\,\varepsilon(1+\varepsilon)}\,\sin\phi_h\,F_{UL}^{\sin\phi_h}+\varepsilon\,\sin(2\phi_h)\,F_{UL}^{\sin 2\phi_h}\right] \\
&\quad +\eta_L\lambda_e\left[\sqrt{1-\varepsilon^2}\,F_{LL}+\sqrt{2\,\varepsilon(1-\varepsilon)}\,\cos\phi_h\,F_{LL}^{\cos\phi_h}\right] \\
&\quad +\eta_t\Big[\varepsilon\,\sin(\phi_h+\phi_\eta)\,F_{UT}^{\sin(\phi_h+\phi_\eta)}+\sin(\phi_h-\phi_\eta)\,F_{UT,T}^{\sin(\phi_h-\phi_\eta)} \\
&\quad +\varepsilon\,\sin(\phi_h-\phi_\eta)\,F_{UT,L}^{\sin(\phi_h-\phi_\eta)}+\varepsilon\,\sin(3\phi_h-\phi_\eta)\,F_{UT}^{\sin(3\phi_h-\phi_\eta)} \\
&\quad +\sqrt{2\,\varepsilon(1+\varepsilon)}\left(\sin\phi_\eta\,F_{UT}^{\sin\phi_\eta}+\sin(2\phi_h-\phi_\eta)\,F_{UT}^{\sin(2\phi_h-\phi_\eta)}\right)\Big] \\
&\quad +\eta_t\,\lambda_e\Big[\sqrt{1-\varepsilon^2}\,\cos(\phi_h-\phi_\eta)\,F_{LT}^{\cos(\phi_h-\phi_\eta)} \\
&\quad +\sqrt{2\,\varepsilon(1-\varepsilon)}\left(\cos\phi_\eta\,F_{LT}^{\cos\phi_\eta}+\cos(2\phi_h-\phi_\eta)\,F_{LT}^{\cos(2\phi_h-\phi_\eta)}\right)\Big]\Bigg\},
\end{aligned}
$$

A. Bacchetta et al. JHEP 0702 (2007) 093

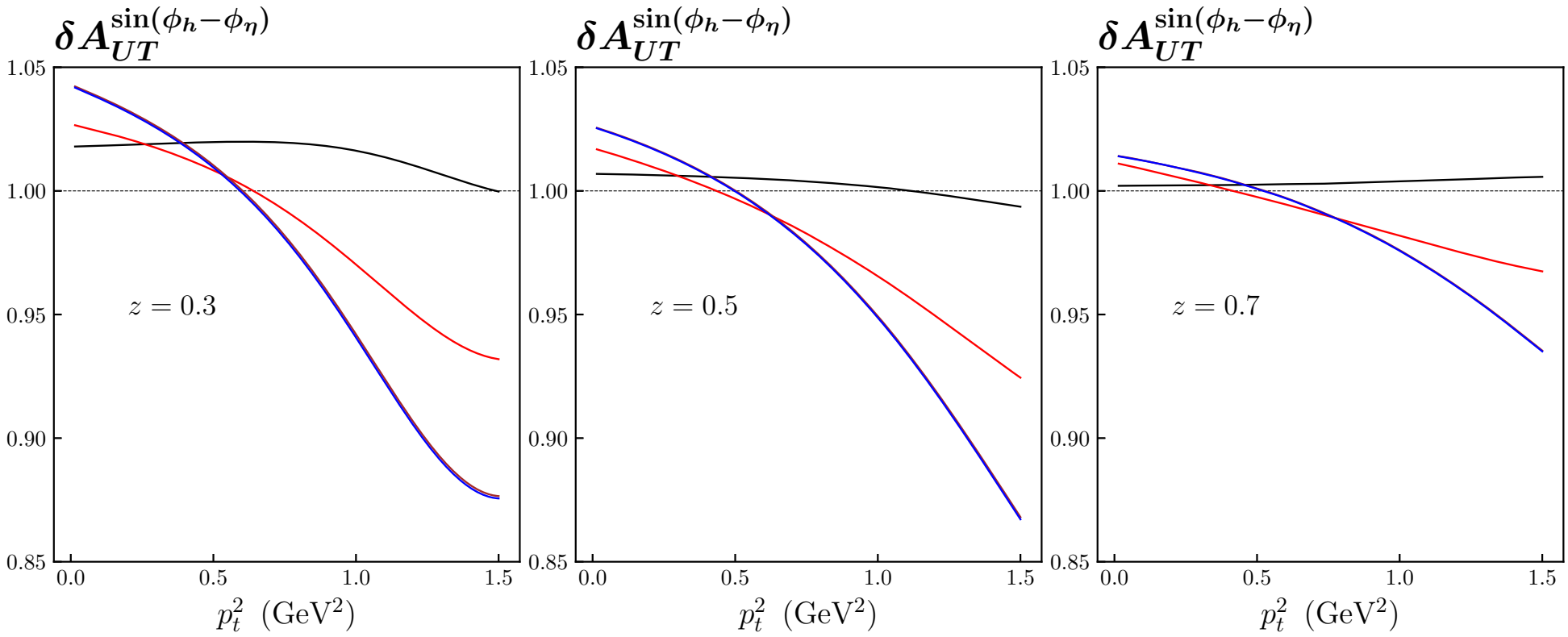
Born cross section

$$
\begin{aligned}
\frac{d^6\sigma_B}{dx\,dy\,d\phi\,dz\,d\phi_h\,dp_t^2} = \frac{\alpha^2}{xy\,Q^2}\,\frac{y^2}{2\,(1-\varepsilon)}\left(1+\frac{\gamma^2}{2x}\right)\Bigg\{ & F_{UU,T} + \varepsilon F_{UU,L} \\
& + \sqrt{2\,\varepsilon(1+\varepsilon)}\,\cos\phi_h\,F_{UU}^{\cos\phi_h} + \varepsilon\cos(2\phi_h)\,F_{UU}^{\cos 2\phi_h} \\
& + \lambda_e\,\sqrt{2\,\varepsilon(1-\varepsilon)}\,\sin\phi_h\,F_{LU}^{\sin\phi_h} + \eta_L\left[\sqrt{2\,\varepsilon(1+\varepsilon)}\,\sin\phi_h\,F_{UL}^{\sin\phi_h} + \varepsilon\,\sin(2\phi_h)\,F_{UL}^{\sin 2\phi_h}\right] \\
& + \eta_L\lambda_e\left[\sqrt{1-\varepsilon^2}\,F_{LL} + \sqrt{2\,\varepsilon(1-\varepsilon)}\,\cos\phi_h\,F_{LL}^{\cos\phi_h}\right] \\
& + \eta_t\Bigg[\varepsilon\,\sin(\phi_h+\phi_\eta)\,F_{UT}^{\sin(\phi_h+\phi_\eta)} + \sin(\phi_h-\phi_\eta)\,F_{UT,T}^{\sin(\phi_h-\phi_\eta)} \\
& \qquad + \varepsilon\,\sin(\phi_h-\phi_\eta)\,F_{UT,L}^{\sin(\phi_h-\phi_\eta)} + \varepsilon\,\sin(3\phi_h-\phi_\eta)\,F_{UT}^{\sin(3\phi_h-\phi_\eta)} \\
& \qquad + \sqrt{2\,\varepsilon(1+\varepsilon)}\left(\sin\phi_\eta\,F_{UT}^{\sin\phi_\eta} + \sin(2\phi_h-\phi_\eta)\,F_{UT}^{\sin(2\phi_h-\phi_\eta)}\right)\Bigg] \\
& + \eta_t\,\lambda_e\Bigg[\sqrt{1-\varepsilon^2}\,\cos(\phi_h-\phi_\eta)\,F_{LT}^{\cos(\phi_h-\phi_\eta)} \\
& \qquad + \sqrt{2\,\varepsilon(1-\varepsilon)}\left(\cos\phi_\eta\,F_{LT}^{\cos\phi_\eta} + \cos(2\phi_h-\phi_\eta)\,F_{LT}^{\cos(2\phi_h-\phi_\eta)}\right)\Bigg]\Bigg\},
\end{aligned}
$$

A. Bacchetta et al. JHEP 0702 (2007) 093

Sivers asymmetries for JLab

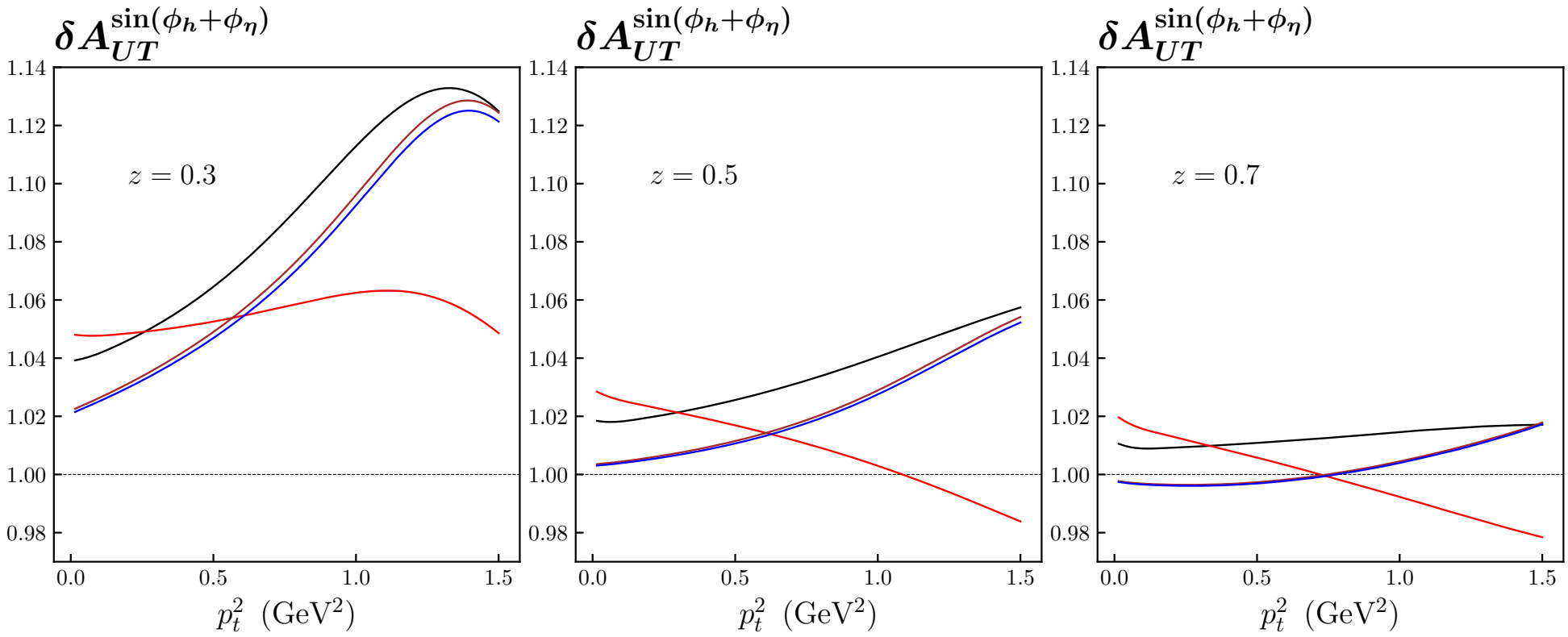
$E_{beam} = 11$ GeV, $Q^2 = 3$ GeV^2, $x = 0.2$



$$\delta A_{UT}^{\sin(\phi_h-\phi_\eta)} = 1 + \frac{A_{UT,\,RC}^{\sin(\phi_h-\phi_\eta)}}{A_{UT,\,B}^{\sin(\phi_h-\phi_\eta)}}$$

Collins asymmetries for Jlab

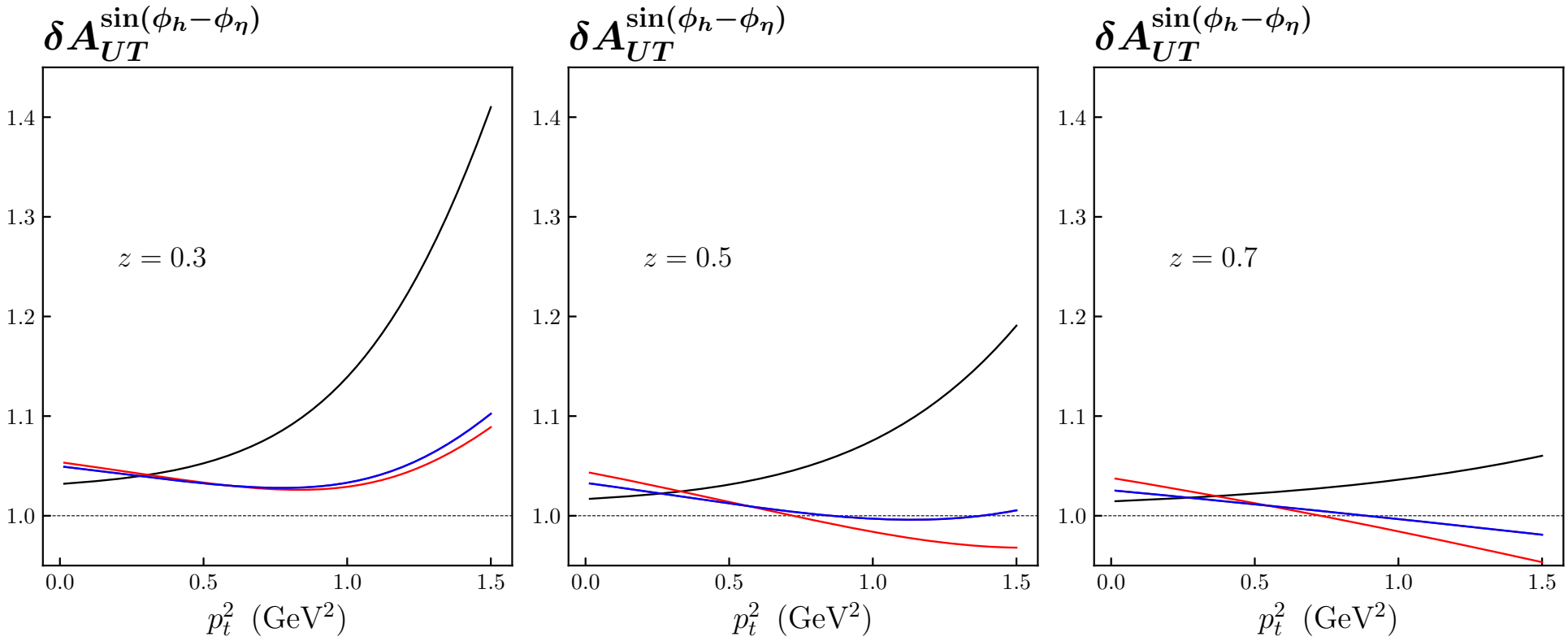
$E_{beam} = 11$ GeV, $Q^2 = 3$ GeV^2, $x = 0.2$



$$\delta A_{UT}^{\sin(\phi_h+\phi_\eta)} = 1 + \frac{A_{UT,\,RC}^{\sin(\phi_h+\phi_\eta)}}{A_{UT,\,B}^{\sin(\phi_h+\phi_\eta)}}$$

Sivers asymmetries for EIC

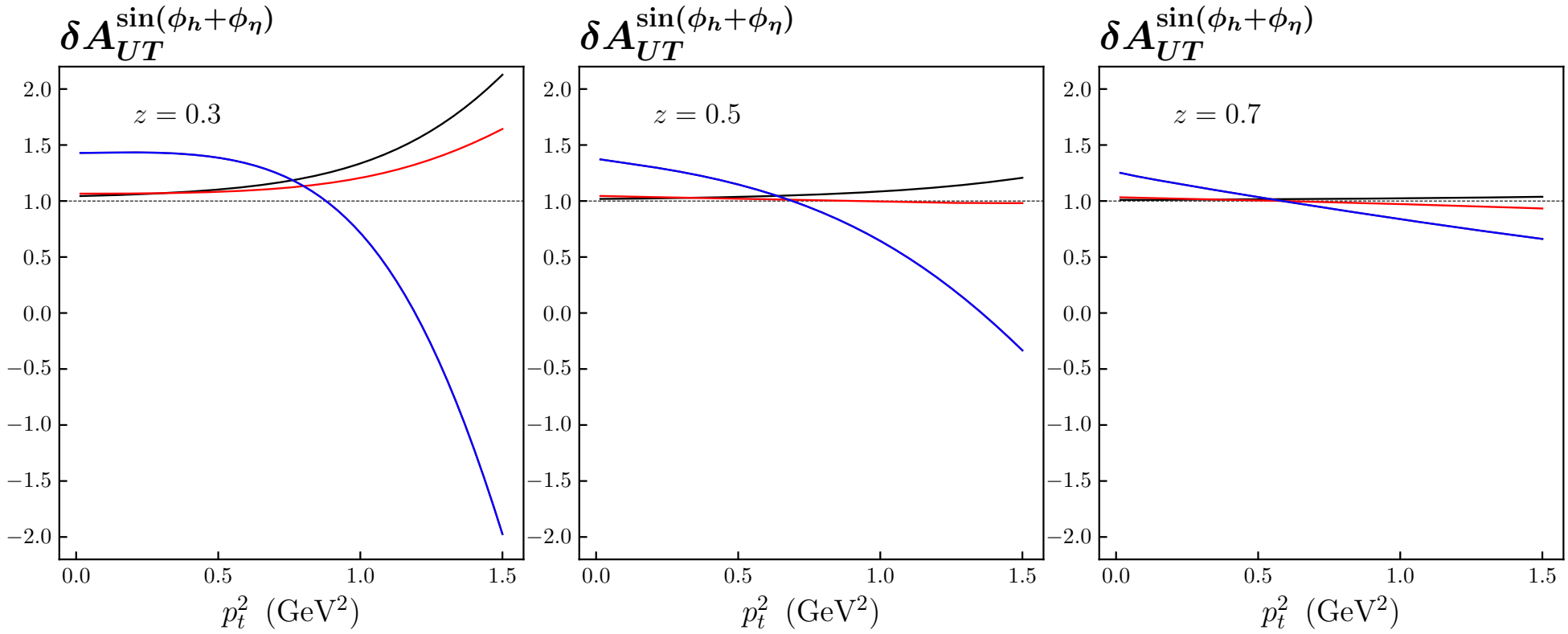
$\sqrt{S} = 28.6$ GeV, $Q^2 = 3$ GeV^2, $x = 0.0073$



$$\delta A_{UT}^{\sin(\phi_h-\phi_\eta)} = 1 + \frac{A_{UT,\,RC}^{\sin(\phi_h-\phi_\eta)}}{A_{UT,\,B}^{\sin(\phi_h-\phi_\eta)}}$$

Collins asymmetries for EIC

$\sqrt{S} = 28.6$ GeV, $Q^2 = 3$ GeV^2, $x = 0.0073$



$$\delta A_{UT}^{\sin(\phi_h+\phi_\eta)} = 1 + \frac{A_{UT,\,RC}^{\sin(\phi_h+\phi_\eta)}}{A_{UT,\,B}^{\sin(\phi_h+\phi_\eta)}}$$

Part VI:

Open Theoretical Questions and Future Directions

Open Points, Previous Version

Exlusive SFs for polarized case *We are working on it, but we will need several models to test model-dependence. Any help will be appreciated.*

SIDIS SFs *We currently implemented WW approach, however, additional cross checks are required for specific regions. Bounds of applicability of WW are needed to be defined and discussed. Additional models would be helpful as well.*

Iteration procedure of RC *We need to decide whether iteration procedure of RC will be used in data analyses. We strongly recommend this (especially for asymmetry measurements) to avoid an additional bias due to RC procedure. The bias is proportional to the difference between the values of Born asymmetries in the given bin: i) finally extracted and ii) used in RC codes. These values coincide by definition when the iteration procedure is used.*

Comparison and agreement between theoretical calculations *We need to complete analytic and numeric comparison to leptonic RC calculated by Tianbo Liu, W. Melnitchouk, Jian-Wei Qiu, and N. Sato (Physical Review D, 104(9), 094033; Journal of High Energy Physics, 2021(11), 1).*

Hadronic corrections *Discuss and decide whether and how non-leptonic corrections (including box diagrams and emission by hadrons) will be calculated.*

Higher order corrections *We need to discuss approaches for higher order corrections, such as exponentiation, electron SFs, etc. Pay specific attention to the region with small* M_x^2.

Monte Carlo *Approaches to MC generators has to be discussed and implemented.*

Open Points, Current Version

Development of the best approximation *Construction of the best approximation in which: i) the order $O(\alpha)$ corrections are calculated exactly, ii) the exclusive RCs are calculated separately, iii) the higher order RCs are computed using leading- and next-to-leading-log contributions, and iv) radiation from hadrons and quarks is incorporated along with radiation from leptons.*

Further development of the hybrid approach *Continued theoretical development of the hybrid approach, including further clarification of the origin of the $\log(1-z)$ term and development of EPM factorization scheme.*

Effects of radiation-induced azimuthal mixing *Detailed numerical investigation of radiation-induced azimuthal mixing for a wide range of asymmetries and other observables in modern SIDIS experiments.*

Evaluation of radiative-correction-induced systematic uncertainties in SIDIS *Quantitative assessment of SIDIS systematic error due to RC, focusing on hadronic SF modeling. A key source is the extension of QCD-based parameterizations into the resonance region, where nonperturbative dynamics prevail, potentially leading to significant biases in RC calculations.*

Electroweak radiative corrections *Extension of the current framework to include electroweak effects, development of a best-approximation formalism incorporating both QED and electroweak radiative corrections, and detailed numerical evaluations for future EIC measurements.*

Extension to additional SIDIS channels *Extension of the theoretical framework and its practical implementation to π^0 and π^--SIDIS measurements.*

Software development for SIDIS radiative-correction studies *Further development of computational tools for SIDIS radiative-correction analyses, including both point-by-point calculation codes (e.g., HAPRAD 3.0) and Monte Carlo event generators suitable for realistic experimental applications.*

Conclusion

- Newly achieved accuracies at JLab and the precision goals of the EIC require renewed attention to radiative-correction calculations and their implementation in data-analysis software.
- The Hybrid approach combines the strengths of traditional and factorized formalisms and provides a pathway toward the most complete SIDIS radiative-correction framework currently achievable.
- Theoretical differences between traditional and factorized approaches are now understood, and the mechanisms responsible for these differences have been identified.
- The EPM factorization scheme provides a physically motivated framework for incorporating exact first-order results into higher-order radiative-correction calculations.
- Radiative azimuthal mixing demonstrates that QED radiation can modify the relation between measured asymmetries and underlying SIDIS structure functions and should be accounted for in precision analyses.

Perspectives

- Completion of a Hybrid radiative-correction framework combining exact $O(\alpha)$ calculations, exclusive radiative tails, higher-order LL/NLL contributions, and radiation from quarks/hadrons within a unified theoretical and computational framework.
- Further development of the Hybrid approach and EPM factorization, including higher-order corrections and studies of factorization-scheme dependence.
- Development of electroweak radiative-correction frameworks for EIC measurements, where electroweak effects become an essential component of high-precision phenomenology.
- Development and implementation of radiative unfolding procedures for spin-dependent SIDIS observables. Since radiative corrections depend on the structure functions being extracted, the problem requires solving an integral equation through iterative reconstruction.
- Quantitative evaluation of radiative-correction-induced systematic uncertainties, with particular emphasis on SIDIS and exclusive structure-function modeling in resonance and other beyond-QCD regions.
- Development of next-generation computational tools for SIDIS radiative-correction studies, including analytical point-by-point calculation codes, SIDIS-specific Monte Carlo generators, and realistic radiated-photon event generation.

Key Message

- The next generation of SIDIS radiative-correction studies should move beyond the calculation of correction factors and toward a unified theoretical and computational framework integrating exact radiative corrections, higher-order resummation, realistic hadronic structure models, and experimental analysis software.

Such a framework will be required to fully exploit the precision potential of Jefferson Lab and the Electron-Ion Collider.

The Hybrid and Exact Physical Matching (EPM) approaches provide a foundation for the development of such a framework.